

Subthreshold Antiproton, K^- , K^+ , and Energetic-Pion Production in Relativistic Nucleus-Nucleus Collisions

A. Shor,^(1,2) E. F. Barasch,⁽³⁾ J. B. Carroll,⁽⁴⁾ T. Hallman,⁽⁵⁾ G. Igo,⁽⁴⁾ G. Kalnins,⁽¹⁾ P. Kirk,⁽⁶⁾ G. F. Krebs,⁽¹⁾ P. Lindstrom,⁽¹⁾ M. A. McMahan,⁽¹⁾ V. Perez-Mendez,⁽¹⁾ S. Trentalange,⁽⁵⁾ F. J. Urban,⁽⁷⁾ and Z. F. Wang⁽⁶⁾

⁽¹⁾Lawrence Berkeley Laboratory, Berkeley, California 94720

⁽²⁾Weizmann Institute of Science, Rehovot 76100, Israel

⁽³⁾Texas A&M University, College Station, Texas 77843

⁽⁴⁾University of California, Los Angeles, California 90024

⁽⁵⁾Johns Hopkins University, Baltimore, Maryland 21218

⁽⁶⁾Louisiana State University, Baton Rouge, Louisiana 70803

⁽⁷⁾Gesellschaft für Schwerionenforschung, D-6100 Darmstadt 11, Federal Republic Germany

(Received 9 August 1989)

We present a measurement of subthreshold antiproton, kaon, and energetic-pion production at 0° for the reactions $^{28}\text{Si}+^{28}\text{Si}$ at 2.0 GeV/nucleon ($E_{\text{available}}/A=0.82$ GeV) and 1.65 GeV/nucleon ($E_{\text{available}}/A=0.70$ GeV), and for $^{20}\text{Ne}+\text{NaF}$ at 2.0 GeV/nucleon. For a given reaction, the particle yields, plotted as a function of the required excitation energy, exhibit a scaling behavior independent of particle species. Implications for collectivity and a common production mechanism are discussed.

PACS numbers: 25.70.Np

The study of subthreshold particle production in relativistic nucleus-nucleus collisions, especially at values of E/A much lower than the threshold for production of the particle in p - p collisions, provides an interesting probe of collective phenomena at large nuclear densities and temperatures. Since conventional sources of particle production hardly contribute at subthreshold energies, subtle phenomena at large nuclear densities may become evident by an enhancement of these particle yields over the expected rates. Subthreshold pion production has been observed in ion-ion collisions at bombarding energies as low as 25 MeV/nucleon,¹ and in collisions of very heavy nuclei at energies down to 138 MeV/nucleon.² Subthreshold K^- production has been detected in nuclear collisions at projectile energies ranging from 2.0 GeV/nucleon down to 1.0 GeV/nucleon.³ At bombarding energies of 1–2 GeV/nucleon, nuclear densities are expected to approach 3–4 times normal nuclear-matter densities,⁴ which may be sufficient for the creation of exotic nuclear states (such as Lee-Wick matter,⁵ pion condensation,⁶ etc.) predicted to occur at large nuclear densities.

Carroll *et al.*⁷ reported the first observation of antiproton production with nuclear beams, in the reaction $^{28}\text{Si}+^{28}\text{Si}$ at 2.1 GeV/nucleon. The \bar{p} yield observed in this measurement is more than 3 orders of magnitude larger than expected on the basis of calculations⁸ that take into account the internal nuclear momentum of the projectile and target nucleons. This same set of calculations is able to reproduce experimental data on subthreshold antiproton production in $p+\text{Cu}$ collisions,⁹ where for bombarding energies ranging from 6 GeV down to 2.9 GeV, the \bar{p} yields decrease by 6 orders of magnitude. The basic ingredient in this calculation is a

parametrization for the internal nuclear momentum based on data from electron scattering,¹⁰ and backward proton production.¹¹ Subthreshold antiproton production has also been observed in Dubna,¹² although at a significantly higher bombarding energy, for the reaction $^{12}\text{C}+^{63}\text{Cu}$ at 3.65 GeV/nucleon ($E_{\text{available}}/A=1.35$ GeV).

We report on a recent experiment in which we measured \bar{p} , K^- , K^+ , and π^- production at 0° in the reaction $^{28}\text{Si}+^{28}\text{Si}$ at 2.0 GeV/nucleon ($E_{\text{available}}/A=0.82$ GeV), and \bar{p} , K^- , and π^- production for $^{28}\text{Si}+^{28}\text{Si}$ at 1.65 GeV/nucleon ($E_{\text{available}}/A=0.70$ GeV) and for $^{20}\text{Ne}+\text{NaF}$ at 2.0 GeV/nucleon. The measurements were made at the Lawrence Berkeley Laboratory Bevalac accelerator on a beam line designed specifically for this measurement. Secondary particles produced at the production target were guided along a spectrometer consisting of two magnetic bends and focusing elements. Detector stations at beam foci included scintillation counters for time-of-flight (TOF) and beam definition, aerogel Cherenkov ($\beta_{\text{thresh}}\sim 0.98c$) and focusing liquid Cherenkov ($\beta_{\text{thresh}}\sim 0.90c$) counters, and at the end station a lead-glass array to measure total deposited energy. The spectrometer, discussed in Ref. 7, will be described elsewhere.¹³ The beam intensity was at 5×10^9 ions/spill, with a production target of thickness corresponding to 50% interaction length for ion-ion collisions.

The data analysis included cuts on the scintillation-counter pulse heights to define the beam and reduce effects due to pileup, as well as cuts on the Cherenkov counters to highlight the kaon and antiproton signals. The data are normalized to previously measured pion cross sections,¹⁴ and corrected for absorption of the secondaries¹⁵ in the production target and detectors and

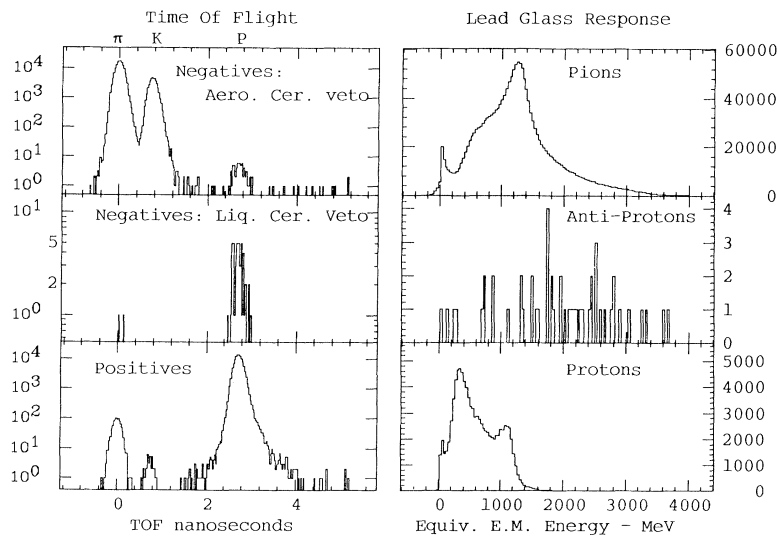


FIG. 1. $^{28}\text{Si}+^{28}\text{Si} \rightarrow$ secondaries at $P=1.9$ GeV/c and 0° . Spectra on left show time of flight for negatives with aerogel Cherenkov veto (top), aerogel and liquid Cherenkov veto (middle), and for positives (bottom). Spectra on the right show lead-glass response for pions (top), antiprotons (middle), and protons (bottom).

for the decay of pions and kaons. The ion energies quoted are the mean energies after taking into account the dE/dX of the ions in the production target.

Figure 1 illustrates the quality of the data for secondaries produced at 1.9 GeV/c and 0° in the reaction $^{28}\text{Si}+^{28}\text{Si}$ at 2.0 GeV/nucleon. The left-hand side of Fig. 1 shows the TOF measurements over the 7-m flight path between detector stations 1 and 2 (relative to pions). At the top left, the TOF spectrum for negative particles not vetoed by the aerogel Cherenkov counters is shown. A clear distinction between the π^- and K^- peaks is seen, and even the \bar{p} peak appears above the background. (Note that the aerogel Cherenkov counters together were only 99.9% efficient to pions.) The middle left plot shows the TOF for events which also did not trigger the liquid Cherenkov counters. A distinct signal containing 50 antiprotons is seen. Out of 2×10^8 events, only two pions survived the Cherenkov vetoes, with no other events (aside from the \bar{p} events) seen over the 50-ns TOF window. These data are taken from two separate runs, with a 50% and a 25% ion-ion interaction-length target, respectively. The ratios of π^- , K^- , and \bar{p} were consistent for these targets. The bottom left figure shows the TOF distribution when the line was tuned for positive secondaries at the same momentum. Peaks corresponding to π^+ , K^+ , and protons appear at the same position in TOF as their negatively charged counterparts. The plots on the right-hand side of Fig. 1 show the total response of the lead-glass array, in units of equivalent electromagnetic energy, for pion, antiproton, and proton events. These distributions of pulse heights differ significantly, with the \bar{p} events depositing more equivalent electromagnetic energy than the proton

events and the pion events at the same momentum. This rules out the possibility that the \bar{p} events are H^- ions.

Figure 2 shows the invariant cross sections for \bar{p} , K^- , K^+ , and π^- production as a function of the particle kinetic energy in the nucleus-nucleus center of mass ($E_{\text{c.m.}}^{\text{kin}}$), for the reaction $^{28}\text{Si}+^{28}\text{Si}$ at 2.0 GeV/nucleon. Also added are several data points from previous π^- and K^- measurements.¹⁴ The π^- and K^- distributions appear to be exponential, i.e., $E d^3\sigma/dP^3 \sim \exp(-E_{\text{c.m.}}^{\text{kin}}/E_0)$, with the slope parameter $E_0=108 \pm 7$ MeV for the π^- , and a similar value of $E_0=103 \pm 7$ MeV for the K^- . The π^- slope parameter, measured here at 0° , is similar to the value of 102 ± 5 MeV measured for pions

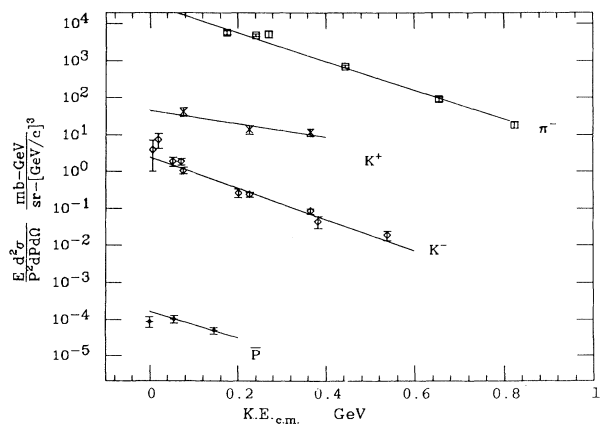


FIG. 2. Invariant cross sections for π^- , K^+ , K^- , and \bar{p} production at 0° for the reaction $^{28}\text{Si}+^{28}\text{Si}$ at 2.0 GeV/nucleon, plotted as a function of particle kinetic energy in the nucleus-nucleus center-of-mass frame ($E_{\text{c.m.}}^{\text{kin}}$).

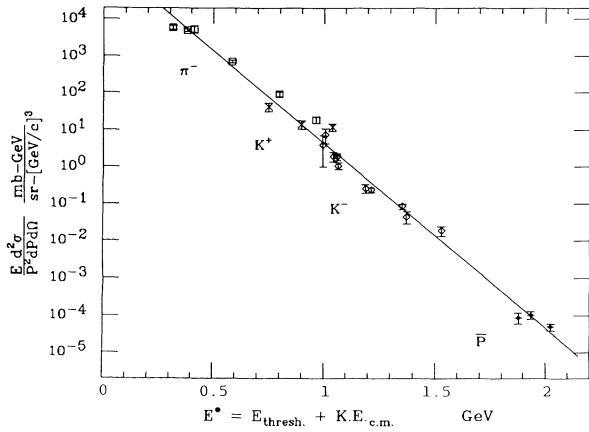


FIG. 3. Invariant cross sections for π^- , K^+ , K^- , and \bar{p} production at 0° for the reaction $^{28}\text{Si}+^{28}\text{Si}$ at 2.0 GeV/nucleon ($E_{\text{available}}/A=0.82$ GeV) plotted as a function of the scaling variable $E^*=E_{\text{thresh}}+E_{\text{c.m.}}^{\text{kin}}$ (same data as in Fig. 2).

at 90° in the c.m. for $\text{Ne}+\text{NaF}$ at 2.1 GeV/nucleon.¹⁶ Our K^+ spectrum, with E_0 of 240 ± 92 MeV, is much flatter than the value of 140 MeV reported by Schnetzer *et al.*¹⁷ for $\text{Ne}+\text{NaF} \rightarrow K^+$ at finite laboratory angles, and may reflect contribution from associated production at small angles. Lastly, our \bar{p} spectrum appears to have a dip at $E_{\text{c.m.}}^{\text{kin}}=0$, although the statistical uncertainties do not make it possible to rule out an exponential falloff. The \bar{p} slope parameter obtained by fitting the two higher-energy data points yields a value for E_0 of 120 ± 50 MeV, similar to E_0 for the π^- and K^- , whereas a value for E_0 of 210 ± 98 MeV is obtained when fitting all three \bar{p} data points. A dip in the \bar{p} spectrum at low \bar{p} c.m. velocities can be expected if the antiprotons are produced in central collisions and where a large number of nucleons exist at midrapidity, since \bar{p} - p annihilation cross sections are large ($\sigma \sim 200$ mb) at low relative velocities.¹⁸

We mention an interesting feature appearing in Fig. 2. At a fixed value of $E_{\text{c.m.}}^{\text{kin}}$, the difference in the invariant cross section between π^- and K^- production is almost identical to the difference between the K^- and \bar{p} production. The threshold excitation energy required for particle production in p - p collisions, denoted by E_{thresh} , is equal to m_π for pion production, $2m_K$ for K^- production, and $2m_p$ for \bar{p} production. The differences in E_{thresh} between pions and K^- , i.e., $2m_K - m_\pi = 0.85$ GeV, is very close in absolute value to the difference in E_{thresh} between K^- and \bar{p} production, i.e., $2m_p - 2m_K = 0.88$ GeV. This feature leads us to the speculation that particle production for this reaction scales with the excitation energy required, independent of particle type.

The above feature is exploited in Fig. 3, which contains the same invariant cross sections for \bar{p} , K^- , K^+ , and π^- as in Fig. 2, but plotted as a function of the variable $E^*=E_{\text{thresh}}+E_{\text{c.m.}}^{\text{kin}}$. [Note that for K^+ , E_{thresh}

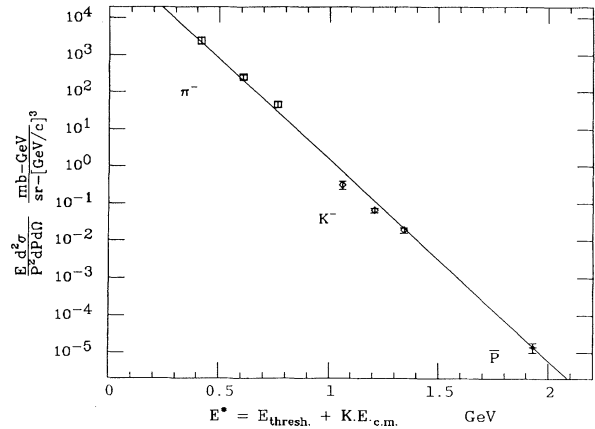


FIG. 4. $^{28}\text{Si}+^{28}\text{Si}$ at 1.65 GeV/nucleon ($E_{\text{available}}/A=0.70$ GeV).

$=(m_\Lambda - m_N) + m_K$]. The particle yields exhibit a scaling in the variable E^* which appears not to be dependent on the particle type. Slight deviations from this scaling are noticeable, although the general trends follow this scaling over 9 orders of magnitude. The deviations from scaling may be due to the difference in final-state interactions at the later stages of the collision process for the different particle types.¹⁹ The scaling behavior is also apparent in Figs. 4 and 5, for π^- , K^- , and \bar{p} production in the reactions $^{28}\text{Si}+^{28}\text{Si}$ at 1.65 GeV/nucleon and for $^{20}\text{Ne}+\text{NaF}$ at 2.0 GeV/nucleon, respectively. The scaling behavior may be parametrized by an exponential function, i.e., $E d^3 \sigma / dP^3 = K_s \exp(-E^*/E_s)$, where the variables E_s and K_s depend on the bombardment energy and the size of the colliding system. The solid curves shown in Figs. 3-5 are fits by eye, and reflect a value of $E_s = 87$ MeV for $\text{Si}+\text{Si}$ at 2 GeV/nucleon, $E_s = 80$ MeV for $\text{Si}+\text{Si}$ at 1.65 GeV/nucleon, and $E_s = 86$ MeV for $\text{Ne}+\text{NaF}$ at 2 GeV/nucleon.

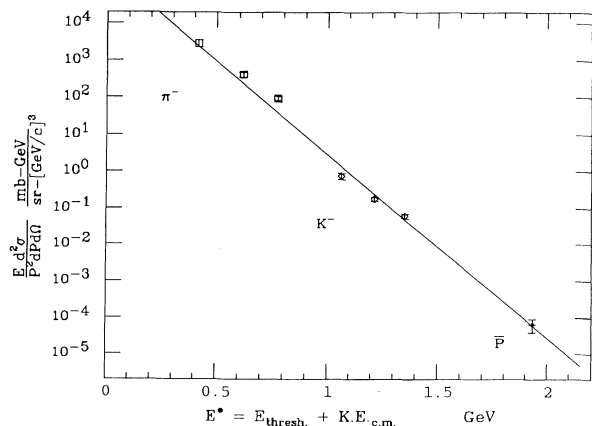


FIG. 5. $^{20}\text{Ne}+\text{NaF}$ at 2.0 GeV/nucleon ($E_{\text{available}}/A=0.82$ GeV).

The scaling behavior observed for particle production in nucleus-nucleus collisions suggests a common production mechanism independent of particle type. This is an important generalization since it would disfavor a mechanism peculiar to one particular particle species, such as the strangeness-exchange mechanism ($Y\pi \rightarrow K^-N$) to explain subthreshold K^- production. Since most of the data in Figs. 3-5 lie beyond the energies accessible to individual $N-N$ collisions (i.e., for values of $E^* > E_{\text{available}}/A$), a collective mechanism for the production of heavy and energetic particles in relativistic nuclear collisions is inferred. An attempt to find scaling for particle production in nucleus-nucleus collisions has also been reported by Baldin *et al.*²⁰ The scaling we observe is similar in nature to that studied by Hagedorn²¹ in high-energy $p-p$ collisions, with the distinction that the scaling reported here is mostly for products that require more energy than is available in the average $N-N$ collision.

We thank the engineering and operations staff of the Bevalac for their support during the experimental program. We thank H. Stroehrer for assistance in setting up the experiment. This work was supported by the Director, Office of Energy Research, Office of High Energy and Nuclear Physics, Nuclear Physics Division of the U.S. Department of Energy under Contracts No. DE-AC03-76S00098, No. DE-FG03-88ER40424, No. DE-FG0288ER40413, No. DE-FG05-88ER40445, and No. DE-AC02-76ER03274.

- ¹G. R. Young *et al.*, Phys. Rev. C **33**, 742 (1986).
- ²J. Miller *et al.*, Phys. Rev. Lett. **58**, 2408 (1987).
- ³J. B. Carroll *et al.*, Nucl. Phys. **A488**, 203c (1988).
- ⁴J. Cugnon, T. Mizutani, and J. Vandermeulen, Nucl. Phys. **A352**, 505 (1981).
- ⁵T. D. Lee, Rev. Mod. Phys. **47**, 267 (1975).
- ⁶A. B. Migdal, Rev. Mod. Phys. **50**, 107 (1978).
- ⁷J. B. Carroll *et al.*, Phys. Rev. Lett. **62**, 1829 (1989).
- ⁸A. Shor, V. Perez-Mendez, and K. Ganezer, LBL Report No. LBL-17067, 1984 (unpublished).
- ⁹D. E. Dorfan *et al.*, Phys. Rev. Lett. **14**, 995 (1965).
- ¹⁰E. J. Moniz *et al.*, Phys. Rev. Lett. **26**, 445 (1971).
- ¹¹J. V. Geaga *et al.*, Phys. Rev. Lett. **45**, 1993 (1980).
- ¹²A. M. Baldin *et al.*, Zh. Eksp. Teor. Fiz. **48**, 127 (1988) [JETP Lett. **47**, 137 (1988)].
- ¹³A. Shor *et al.* (unpublished).
- ¹⁴E. F. Barasch, thesis, University of California, Davis, 1986 (unpublished).
- ¹⁵K. Nakamura *et al.*, Phys. Rev. Lett. **52**, 731 (1984).
- ¹⁶S. Nagamiya *et al.*, Phys. Rev. C **24**, 971 (1981).
- ¹⁷S. Schnetzer *et al.*, Phys. Rev. Lett. **49**, 989 (1982).
- ¹⁸Particle Data Group, G. P. Yost *et al.*, Phys. Lett. B **204**, 127 (1988).
- ¹⁹S. Nagamiya, Phys. Rev. Lett. **49**, 1383 (1982).
- ²⁰A. Kurepin *et al.*, in *Proceedings of the Eighth International Seminar on High Energy Physics Problems, Dubna, 1986*, edited by T. Y. Zhubitskaya and E. V. Ivashkevich (Joint Institute of Nuclear Study, Dubna, 1987), Vol. 1, p. 273; A. M. Baldin *et al.*, Dubna Internal Report No. D2-82-568, 1982 (unpublished).
- ²¹R. Hagedorn, Rev. Nuovo Cimento **6**, 1 (1982).